American Journal of Analytical Chemistry, 2011, 2, 9-17
doi:10.4236/ajac.2011.21002 Published Online February 2011 (http://www.SciRP.org/journal/ajac)

Elucidation of Abnormal Potential Responses of Cation-Selective Electrodes with Solid-State Membranes to Aqueous Solutions of $CuCl_2$ and CdI_2

Yoshihiro Kudo[1]*, Daisuke Todoroki[2], Nobukazu Suzuki[2], Naoki Horiuchi[1], Shoichi Katsuta[1], Yasuyuki Takeda[1]
[1]*Graduate School of Science, Chiba University, Chiba, Japan*
[2]*Department of Chemistry, Faculty of Science, Chiba University, Chiba, Japan*
E-mail: iakudo@faculty.chiba-u.jp
Received September 9, 2010; *revised January* 5, 2011; *accepted January* 10, 2011

Abstract

An empirical solution to abnormal potential responses, showing peaks of emf, of commercial Cu^{2+}- and Cd^{2+}-selective electrodes with solid-state membranes was proposed for aqueous solutions of $CuCl_2$ and CdI_2. The two-step processes of $M^{n+} + Y^{n-}$ (s: solid phase) $\rightleftharpoons$ MY(s) and MY(s) + $2X^- \rightleftharpoons X_2MY^{2-}$(s) ($n$ = 1, 2) at a test solution/electrode-interface were considered as a model. Here, M^{n+}, Y^{n-}, and X^- refer to a divalent or univalent cation, functional groups of electrode materials, and a halide ion ($X^- = Cl^-, Br^-, I^-$), respectively. By applying electrochemical potentials to these processes at n = 2, we derived an equation. Regression analyses based on the equation reproduced well the plots of emf versus log 2(*$[M]_t$) for the Cd(II) and Cu(II) systems: *$[M]_t$ denotes a total concentration of species relevant to M^{2+} in a bulk of the aqueous solution. Also, as an apparent selectivity coefficient (K_s) we obtained log $K_s(CdBr_2) = 4.28 \pm 0.22$, log $K_s(CdI_2) = 6.98 \pm 0.05$, log $K_s(CuCl_2) = 3.96 \pm 0.09$, and log $K_s(CuBr_2) = 11.4$ at 25˚C. The magnitude in $-\log K_s$ reflected that in the logarithmic solubility product, log {*$[M^{2+}]$(*$[X^-])^2$}, for bulk water, where *$[M^{2+}]$ or *$[X^-]$ denotes a molar concentration of the bulk solution of M^{2+} or X^- at equilibrium, respectively. Moreover, a mixture of $CuSO_4$ with NaCl at the molar ratio of 1:1 yielded a plot similar to that of $CuCl_2$.

Keywords: Cation-Selective Electrode, Solid-State Membranes, Potential Response, Solubility Product, Potentiometry

1. Introduction

Many ion-pair (or complex) formation constants of divalent metal salts (MX_2) in water (w) have been determined so far [1-4]. In the course of potentiometric determination of these constants for CdI_2 and $CdBr_2$ in a bulk w by using a commercial Cd^{2+} electrode with a solid-state membrane [4], plots of the emf versus log 2(*$[CdX_2]_t$) gave peaks, where *$[CdX_2]_t$ (= *$[Cd]_t$) denotes a total concentration of CdX_2 in the bulk w. Especially, as shown in **Figure 1** of the previous paper [4], a slope of the plot for the CdI_2 system was positive in the lower range of log 2(*$[CdI_2]_t$), while it was negative in its higher range. As a result, the Cd^{2+} electrode could not be used for the determination of the formation constants. Such plots with the peaks, namely Λ-shaped plots, have been reported in the cases of potential responses of cation-selective electrodes with liquid membranes to some anions, such as F^-, SCN^- and ClO_4^- [5-7]. Also, similar potential responses were observed in the case of a commercial Cu^{2+} electrode with a solid-state membrane, when the ion-pair formation of $CuCl_2$ in w had been studied for the application to solvent-extraction experiments of some Cu(II) salts by crown compounds into 1,2-dichloroethane. The same application has been reported for Cd(II) salts [8].

However, it is difficult to see some models proposed for elucidating the potential responses of the electrodes with the liquid membranes [5,7-12] and its elucidation seems to be unclear [5,7]. The Nicolsky- or Nicolsky-Eisenman-type equation [9,13] does not reproduce the Λ-shaped potential responses. Also, some equations derived from the inverted-Nernstian response model based on the complexation of ionophores with primary and/or secondary ions [11,12] can not clearly express the responses.

In the present paper, we tried the reproduction of the above plots by introducing a model with two-step processes around the electrode/solution interface, in addition to ion-pair formation. Applying an electrochemical potential to these processes, we derived an equation and thereby reproduced the Λ-shaped plot of the CdI_2 system. Also, plots similar to that of the CdX_2 system (X = Cl to I) were observed in CuX_2 (Cl, Br) and CaX_2 systems (Cl to I). Furthermore, properties of commercial ISEs, Cd^{2+} and Cu^{2+} electrodes with solid-state membranes and Ca^{2+} one with a liquid membrane, were examined using an apparent selectivity coefficient (K_s) obtained at 25˚C from the analyses of these plots by the derived equation. Additionally, the equation was extended to potential responses of M^+-selective electrodes.

2. Experimental

2.1. Chemicals

Purities of $CuCl_2 \cdot 2H_2O$ (guaranteed pure, Kanto), $CuBr_2$ (guaranteed pure, Kanto), $CuSO_4 \cdot 5H_2O$ (guaranteed pure, Wako), $CaBr_2$ (98%, degree of hydration ≤ 1, Aldrich), and $CaI_2 \cdot nH_2O$ (99.5%, n = 3 to 4, Wako) were determined by chelatometric titration with EDTA [4]. NaCl (99.99%, Wako) and KCl (≥ 99.8%, Kanto) were prepared from the procedures described in a previous paper [14]. Other chemicals were used without any purification. Tap water was distilled once and then deionized by passing through a Milli-Q Lab System. This water was used for preparing all aqueous solutions.

2.2. Instruments

As the commercial ISEs, the Cu^{2+} electrode (Horiba, type 8006-10C) with the solid-state membrane and the Ca^{2+} electrode (Horiba, type 8203-10C) with the liquid membrane were employed. The emf values were measured with a Horiba pH/ion meter F23 equipped with the ISE and a reference electrode (Horiba, type 2565A-10T) [4, 15].

2.3. Emf Measurements

Emf values were measured at 25 ± 0.3˚C in the following cell: Ag│AgCl│0.1 $mol \cdot L^{-1}$ KCl or NaCl │1 $mol \cdot L^{-1}$ KNO_3│test solution│ISE [4]. As the test solutions, aqueous solutions of $CuCl_2$, $CuBr_2$, $CaBr_2$, CaI_2, NaCl, and mixtures of $CuSO_4$ with NaCl were used. As a result of computation by the Henderson equation, the liquid junction potentials (< 3 mV) at the 1 $mol \cdot L^{-1}$ KNO_3│test solution-interface were neglected [4]: this shows that the aqueous solution of 1 $mol \cdot L^{-1}$ KNO_3 adequately functions as a salt bridge. The mixtures were prepared by mixing 0.5006 $mol \cdot L^{-1}$ of $CuSO_4$ with 0.5007 $mol \cdot L^{-1}$ of NaCl at given volume-ratios.

3. Results and Discussion

3.1. Log *$[X]_t$-Dependence of Emf

Figure 1 shows the dependence of the experimental emf-values on the log *$[X]_t$ ones for (a) the CuX_2 (X = Cl, Br), (b) CdX_2, and CaX_2 (Br, I) systems. Here, *$[X]_t$ denotes a total concentration of species relevant to X^- in the bulk w and equals 2(*$[MX_2]_t$). Therefore, this relation indicates that the plots of emf versus log *$[X]_t$ are actually equivalent with those versus log {2(*$[MX_2]_t$)} in **Figures 1** and **2** {see Equations (10) & (10a)} and accordingly the plots become showed the log (*$[MX_2]_t$)-dependence of emf with a constant deviation of log 2. Except for the $CuBr_2$ system, these plots had positive slopes of 26 to 37 mV/decade in the lower log *$[X]_t$ ranges, showing the Nernstian responses of the electrodes, and then became the lower or negative slopes in the higher ranges. Only the negative slope was observed for the $CuBr_2$ system (open diamond in **Figure 1(a)**) under the present experimental conditions. Its value shows that the Cu^{2+} electrode used can act as a selective electrode for Br^-, as suggested on its instruction manual. Also, the fact means that, even in the lower log *$[X]_t$ range, its solid-state membrane more-preferentially interacts with Br^- than does with Cu^{2+}.

Peaks in emf seemed to shift into the higher values of log *$[X]_t$ in the order X = I < Br < Cl for the MX_2 systems employed (**Figure 1**). In going from X = Br to I, their peaks were well-defined for the Cd(II) system (**Figure 1(b)**), while, in going from Cl to Br, those was less-defined for the Cu(II) system (**Figure 1(a)**).

3.2. Contribution of Ion-Pair Formation to the Plots of Emf versus Log *$[X]_t$

Only the Nernstian slopes of about 30 mV/decade have been observed in calibration curves for the aqueous solutions of $Cd(NO_3)_2$ with 0.1 $mol \cdot L^{-1}$ KNO_3 (as an adjuster of ionic strength, I), $CuSO_4$ with 0.1 $mol \cdot L^{-1}$ KNO_3, and $CaCl_2$ with 0.1 $mol \cdot L^{-1}$ KCl, as shown in the figures of their instruction manuals. These facts indicate that the ion-pair (or complex) formation for these salts at I = 0.1 $mol \cdot L^{-1}$ with KX (X^- = NO_3^-, Cl^-) does not practically

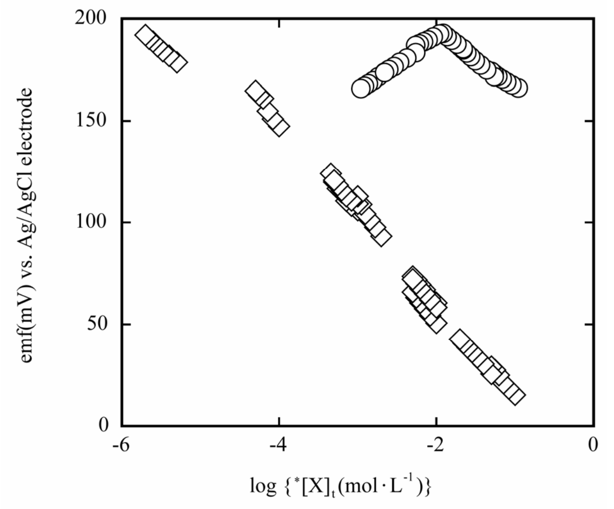

(a)

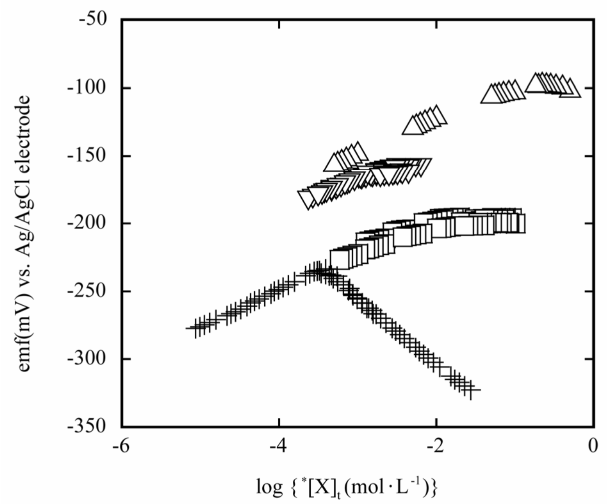

(b)

Figure 1. Plots of emf versus log *[X]$_t$ for the CuX$_2$ (X = Cl : ○; Br: ◊), CdX$_2$ {Br: □; I: + [4]}, and CaX$_2$ systems (Br: Δ; I:∇).

influence the linearity of the calibration curves. For example, the calibration curve for the aqueous solution of $CuSO_4$ is expressed as emf = $a + b$ log *[Cu^{2+}] = $a + b$ log [*[Cu]$_t$/{1 + K_{CuSO4}(*[SO_4^{2-}])}] ≈ $a' + b$ log *[Cu]$_t$, being the experimental equation of the calibration curve, where K_{CuSO4} = *[$CuSO_4$]/(*[Cu^{2+}])*[SO_4^{2-}] (≤ 251 mol·L^{-1} [16]), *[Cu]$_t$ = *[Cu^{2+}] + *[$CuSO_4$], and $a' \equiv a - b$ log {1 + K_{CuSO4}(*[SO_4^{2-}])}. The symbol *[Cu^{2+}] or *[$CuSO_4$] refers to a molar concentration of Cu^{2+} or $CuSO_4$ in the bulk w at equilibrium, respectively. This relation of emf to log *[Cu]$_t$ suggests that, in spite of the larger K_{CuSO4} value, the condition of either 1 >> K_{CuSO4} (*[SO_4^{2-}]) or 1 + K_{CuSO4}(*[SO_4^{2-}]) ≈ constant holds actually. In other words, the condition indicates that the

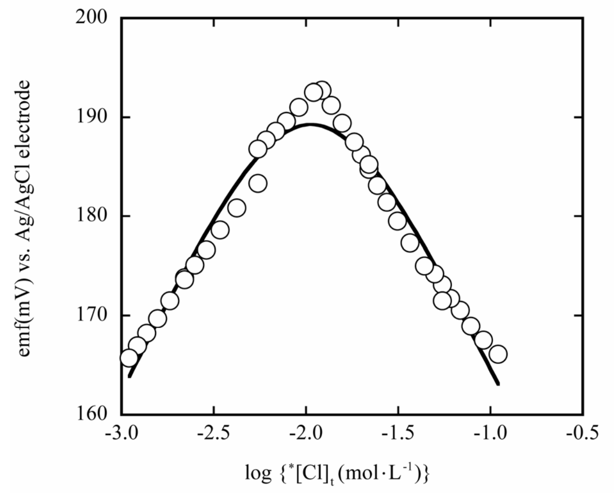

Figure 2. Plots of emf versus log *[Cl]$_t$ for the $CuCl_2$ system.

ion-pair formation is less effective for the *b* (slope) value of the calibration curve, while it is somewhat effective for the *a* (intercept) value. Also, it is predicted that its effects on the $Cd(NO_3)_2$ and $CaCl_2$ (K_{CaCl} ≤ 41 mol·L^{-1} at 25˚C [4,15]) solutions are lower than that on the $CuSO_4$ solution. In comparison with the K_{CuSO_4} value(s) [16], the above condition should hold for the CdI_2 system with K_{CdI} ≤ 308 mol·L^{-1} at 25˚C [4]: emf = $a + b$ log *[Cd^{2+}] ≈ $a + b$ log [*[Cd]$_t$/{1 + K_{CdI}(*[I^-])}] ≈ $a' + b$ log *[Cd]$_t$ in the log *[Cd]$_t$ range of –5 to –2 at least [4], where *[Cd]$_t$ ≈ *[Cd^{2+}] + *[CdI^+] = *[Cd^{2+}] + K_{CdI}(*[Cd^{2+}])*[I^-]. These results indicate that the condition of 1 >> K_{MX}(*[X^-]) holds for the present $M^{II}X_n$ (n = 1, 2) systems. The same discussion should be true of *[X]$_t$ because of *[X]$_t$ = 2(*[M]$_t$). The above results may be similar to that clarified by Kakiuchi: when the volume ratio of the membrane to the test solution approaches zero, the potential generated at its interface does not affected by the ion-pair formation in the membrane [17].

3.3. Semi-Theoretical Treatment for Potential Response of M^{2+}-Selective Electrodes to X^-

We considered here the following three processes around the test solution/ISE-interface for the electrode response, neglecting the formation of MX_2.

$$M^{2+} + Y^{2-}(\text{s : solid phase}) \rightleftharpoons MY(\text{s}) \quad (1)$$

$$MY(\text{s}) + 2X^- \rightleftharpoons X_2MY^{2-}(\text{s}) \quad (2)$$

$$M^{2+} + X^- \rightleftharpoons MX^+ \quad (3)$$

Here, taking the easy formation of four-coordinated Cu(II) and Cd(II) complexes with X^- into account, we neglected the formation of XMY^- species in Equation (2).

For the overall process of the electrode processes (1) and (2), therefore, the corresponding equilibrium-constant was defined as

$$K = \left[X_2MY^{2-}\right]_s \Big/ \left(\left[M^{2+}\right]\left[Y^{2-}\right]_s\left[X^-\right]^2\right) = \left(\left[X_2MY^{2-}\right]_s \Big/ \left[Y^{2-}\right]_s\right) \Big/ \left[M^{2+}\right]\left[X^-\right]^2 \quad (4)$$

and those for the process (1) to (3) were

$$K_1 = [MY]_s \Big/ \left[M^{2+}\right]\left[Y^{2-}\right]_s, \quad (1a)$$

$$K_2 = \left[X_2MY^{2-}\right]_s \Big/ [MY]_s\left[X^-\right]^2 \quad (2a)$$

and

$$K_{MX} = \left[MX^+\right] \Big/ \left[M^{2+}\right]\left[X^-\right] = {}^*\left[MX^+\right] \Big/ {}^*\left[M^{2+}\right]\left({}^*\left[X^-\right]\right), \quad (3a)$$

where [*j*] and *[*j*] refer to molar concentrations of species *j* (= M^{2+}, MX^+, X^-) around the electrode interface and *j* in a bulk of the test solution, respectively. The subscript (or superscript) "s" means the solid phase of the electrode and can be replaced by "o", which means an organic phase, for the liquid membrane ISE. We used here the molar concentrations instead of the activities, because they render the theoretical treatment complicated and also the experimental calibration curves keep linearity in the ranges of 10^{-5} (or 10^{-6}) to 10^{-1} mol·L^{-1} for Cu^{2+} in w, 10^{-6} to 10^{-1} mol·L^{-1} for Cd^{2+}, and 2.5 × 10^{-5} to 0.25 (or 1) mol·L^{-1} for Ca^{2+}, as shown in the specifications [18-20] of a Website.

The above electrode processes (1) and (2) at the interface were also expressed by electrochemical potentials ($\bar{\mu}$) as follows.

$$\bar{\mu}_M + \bar{\mu}_Y^s = \bar{\mu}_{MY}^s \quad (1b)$$

$$\bar{\mu}_{MY}^s + 2\bar{\mu}_X = \bar{\mu}_{X2MY}^s \quad (2b)$$

Arranging Equations (1b) and (2b) by the properties of $\bar{\mu}$ [21], we have easily

$$\phi_Y^s - \phi_M = \frac{\mu_Y^{0s} + \mu_M^0 - \mu_{MY}^{0s}}{2F} + \frac{RT}{2F}\ln\left[M^{2+}\right] \quad (5)$$

$$= \Delta\phi_{Y/M}^0 + \frac{RT}{2F}\ln\left[M^{2+}\right] \quad (5a)$$

$$\phi_{X2MY}^s - \phi_X = \frac{\mu_{X2MY}^{0s} - 2\mu_X^0 - \mu_{MY}^{0s}}{2F} + \frac{RT}{2F}\ln K_2 \quad (6)$$

$$= \Delta\phi_{X2MY/X}^0 + \frac{RT}{2F}\ln K_2. \quad (6a)$$

Here, ϕ_j, $\Delta\phi_{j/j'}^0$, and μ_j^0 denote an inner potential for the species *j* (= M^{2+}, Y^{2-}, X_2MY^{2-}) in each phase, a standard electrode potential, and a standard chemical potential corresponding to *j*, respectively. *R*, *T* and *F* have the usual meanings. By the sum of Equations (5a) and (6a), we could express the emf value in question as

$$\text{emf} \approx \Delta\phi_{Y/M}^0 + \frac{RT}{2F}\ln\left[M^{2+}\right] + \Delta\phi_{X2MY/X}^0 + \frac{RT}{2F}\ln K_2. \quad (7)$$

Also, the following relations were derived from mass balance equations around the test solution/electrode-interface.

$$[M]_t = \left[M^{2+}\right] + \left[MX^+\right] + [MY]_s + \left[X_2MY^{2-}\right]_s \approx \left[M^{2+}\right] + \left[MX^+\right] + \left[X_2MY^{2-}\right]_s \approx \left[M^{2+}\right]\left(1 + K\left[Y^{2-}\right]_s\left[X^-\right]^2\right) \quad (8)$$

by assuming that 1 >> $K_2[X^-]^2$ and then 1 + $K[Y^{2-}]_s[X^-]^2$ >> $K_{MX}[X^-]$ (see above for 1 >> $K_{MX}[X^-]$) and

$$[X]_t = \left[X^-\right] + \left[MX^+\right] + 2\left[X_2MY^{2-}\right]_s = \left[X^-\right]\left(1 + K_{MX}\left[M^{2+}\right] + 2K\left[Y^{2-}\right]_s\left[M^{2+}\right]\left[X^-\right]\right) = \left[X^-\right]g \quad (8a)$$

with $g = 1 + K_{MX}[M^{2+}] + 2K[Y^{2-}]_s[M^{2+}][X^-]$. Rearranging Equation (8) as

$$\left[M^{2+}\right] = \frac{{}^*[M]_t D_M}{1 + K\left[Y^{2-}\right]_s\left(\left[X^-\right]_t/g\right)^2} = \frac{{}^*[M]_t D_M}{1 + K\left[Y^{2-}\right]_s\left(D_X/g\right)^2\left({}^*\left[X^-\right]_t\right)^2} \quad (9)$$

with $D_M = [M]_t/{}^*[M]_t$ {≈ ($[M^{2+}] + [MX^+] + [MY]_s + [X_2MY^{2-}]_s$)/($*[M^{2+}] + *[MX^+]$)} and $D_X = [X]_t/{}^*[X]_t$ {≈ ($[X^-] + [MX^+] + 2[X_2MY^{2-}]_s$)/($*[X^-] + *[MX^+]$)} and then introducing Equation (9) into Equation (7), we have easily

$$\text{emf} \approx \Delta\phi_{Y/M}^0 + \Delta\phi_{X2MY/X}^0 + \frac{RT}{2F}\ln\frac{K_m}{2} + \frac{RT}{2F}\ln{}^*[X]_t - \frac{RT}{2F}\ln\left\{1 + K_s\left({}^*[X]_t\right)^2\right\} \quad (10)$$

$$= \Delta\phi_{Y/M}^0 + \Delta\phi_{X2MY/X}^0 + \frac{RT}{2F}\ln K_m + \frac{RT}{2F}\ln{}^*[M]_t - \frac{RT}{2F}\ln\left\{1 + 4K_s\left({}^*[M]_t\right)^2\right\} \quad (10a)$$

with $D_MK_2 = K_m$, $K[Y^{2-}]_s(D_X/g)^2$ {= $K[Y^{2-}]_s([X^-]/{}^*[X]_t)^2$ = $([X_2MY^{2-}]_s/[M^{2+}])/({}^*[X]_t)^2$} = K_s, and $*[X]_t = 2(*[M]_t)$ {= $2(*[MX_2]_t)$}. Here, the D_M and D_X values like distribution ratios at the test solution/electrode-interface were assumed to be much smaller than unity and the term

D_X/g is dimensionless.

Using emf = $A + B \log *[X]_t + C \log \{1 + K_s(*[X]_t)^2\}$, we can immediately analyze the plots of emf versus log $*[X]_t$ by a non-linear regression: the alphabet A to C mean $A = \Delta\phi^0_{Y/M} + \Delta\phi^0_{X2MY/X} + (RT/2F)\ln(K_m/2)$, $B = 2.303RT/2F$ for log $*[X]_t$, and $C = -2.303RT/2F$ in Equation (10). Considering asymmetry of the plots (see **Figures 1(b)** and **2**), we distinguished here B from C and computed their values together with estimating whether they are positive or negative. In Equation (10), K_s will act as the potentiometric selectivity coefficient (k^{pot}), usually-described for a glass electrode [21], of the anion X^- against M^{2+}. Namely, like k^{pot}, the larger the K_s value is, the larger the interference of X^- to the potential response of the electrode becomes.

According to the instruction manual, it has been described that the Cu^{2+} concentration detected by the Cu^{2+} electrode decreases in the presence of Cl^-, Br^-, or I^-. From Equation (10a), a difference in emf between $2*[M]_t$ ($= *[X]_t$) = 0 and x is expressed as emf(x) – emf(0) = $B \ln\{*[Cu]_t(x)/*[Cu]_t(0)\} + C \ln(1 + K_s x^2)$. When experimentally $*[Cu]_t(x)/*[Cu]_t(0) \approx 1$, this equation becomes emf(x) ≈ emf(0) + $C \ln(1 + K_s x^2)$. Therefore, the relation of emf(0) ≠ emf(x) is obtained: namely the inequality of emf(x) < emf(0) should hold, because $C < 0$ and $\ln(1 + K_s x^2) > 0$. This fact, emf(x) < emf(0), also indicates that, considering the calibration curve of emf = $a' + b \log *[Cu]_t$ with $b > 0$ (see **3.2**), $10^{-\{emf(0) - emf(x)\}/b} = *[Cu]_t(x)/*[Cu]_t(0) < 1$ must hold. This result that $*[Cu]_t(x)$ becomes smaller than $*[Cu]_t(0)$ is in accord with that described above. Thus, the above description in the manual is well explained in terms of Equation (10a).

An equation similar to Equation (10) was obtained for the M^+X^- system:

$$\text{emf} \approx A + B\log *[M]_t + C\log\left\{1 + K_s\left(*[M]_t\right)^2\right\} \quad (11)$$

with $A = \Delta\phi^0_{Y/M} + \Delta\phi^0_{X2MY/X} + (RT/2F)\ln(K_m D_M)$, $B = 2.303RT/F$, and $C = -2.303RT/F$, and $K_s = K[Y^-]_s(D_M/g)^2$. Here, taking account of the processes, $M^+ + Y^-(s) \rightleftharpoons MY(s)$ and $M^+ + X^- \rightleftharpoons MX^0$ instead of Equations (1) and (3), we modified the $\Delta\phi^0_{Y/M}$, D_M, and g terms.

3.4. Reproduction of Plots of Emf versus Log $*[X]_t$

A curve in **Figure 2** shows the semi-theoretical curve for the $CuCl_2$ system obtained from the above treatment. Thus, the plot was reproduced well. The same analyses also yielded results similar to those for other plots. These A, B, C, and log K_s values are summarized in **Table 1**.

The curve (**Figure 2**) was resolved into emf_M and emf_X, where emf = $emf_M + emf_X$, indicating $emf_{Cu} = A + B \log *[Cl]_t$ and $emf_{Cl} = C \log\{1 + K_s(*[Cl]_t)^2\}$ with M = Cu and X = Cl, from Equation (10). Their emf values are listed in **Table 2** with some experimental emf values (emf^{found}). One can see easily the sum of the two emf values, emf_{Cu} and emf_{Cl}, well reproduces the emf^{found} values within error of about |2| mV. Additionally, **Table 2** shows that the emf_{Cl} values depress the Nernstian response of the Cu^{2+} electrode in the log $*[Cl]_t$ range more than –2. Other experimental plots of the emf versus log $*[X]_t$ were resolved similarly, except for the $CuBr_2$ system. As **Figure 1(a)** shows, the Nernstian response for Cu^{2+} in the presence of Br^- in w was not observed at all. Hence, its plot was analyzed by using the following linear equation: emf ≈ $emf_{Br} = A + C \log K_s + (B + 2C)\log *[Br]_t = A' + C' \log *[Br]_t$ under the condition of $K_s >> (*[Br]_t)^{-2}$ ($\approx 10^{11.4}$ $mol^{-2}\cdot L^2$ at the experimental minimum $*[Br]_t$), namely $1 << K_s(*[Br]_t)^2$ in Equation (10).

The same regression analyses were performed by using Equation (10) for the potential response of the Ca^{2+} electrode with the liquid membrane. The thus-obtained results are listed in **Table 1**. The values obtained seem to be comparable with those for the solid-state electrodes.

3.5. Addition of NaCl into Aqueous Solution of $CuSO_4$

Figure 3 shows a variation of the emf values for mixtures of aqueous solutions of $CuSO_4$ with those of NaCl at $*[NaCl]_t/*[CuSO_4]_t$ = 1.00 (open circles) and 3.00 (open squares). Obviously, the emf-versus-log $*[CuSO_4]_t$ plots were spread out a range of negative slopes with an increase in amount of NaCl. This shows any interferences of Cl^- against the potential response of the Cu^{2+}

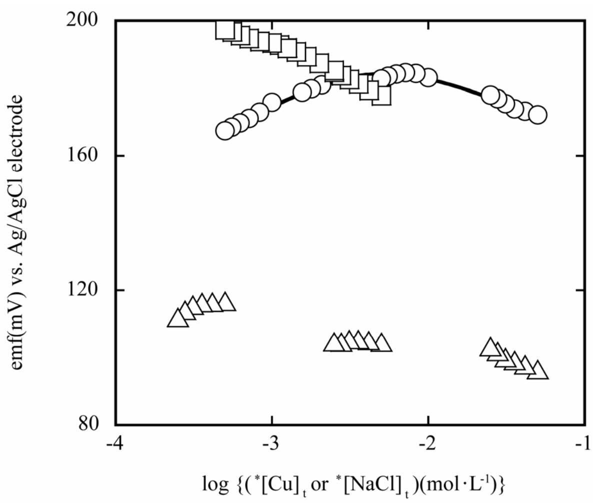

Figure 3. Plots of emf versus log $*[Cu]_t$ for the mixtures of $CuSO_4$ with NaCl at $*[NaCl]_t/*[CuSO_4]_t$ = 1.00 (○) and 3.00 (□). The plot with open triangles shows a potential response of the Cu^{2+} electrode to the aqueous solution of NaCl.

Table 1. Some electrochemical parameters obtained from the plots of emf versus log 2(*[MX_2]$_t$) at 25˚C.

MX_2	Membrane type	A (mV)	B (mV/decade)	C (mV/decade)	log K_s	R
$CdBr_2$	Solid-state	−143 ± 7	26 ± 2	−13 ± 1	4.2_8± 0.2_2	0.959
CdI_2	Solid-state	−104 ± 7	35 ± 2	−44 ± 1	6.98 ± 0.05	0.994
$CuCl_2$	Solid-state	274 ± 7	37 ± 3	−37 ± 1	3.96 ± 0.09	0.981
$CuBr_2$	Solid-state	−19 ± 3[a]	---[b]	−40 ± 1[a]	11.4[c]	0.987
$CaBr_2$	Liquid	−69 ± 1	26 ± 1	−16 ± 2	1.8_7 ± 0.1_9	0.999
CaI_2	Liquid	−76 ± 17	29 ± 5	−11 ± 2	6.0_0 ± 0.3_8	0.976

[a]Determined by using emf = A' + C' log *[X]$_t$. [b]The Nernstian response was not observed. [c]Estimated from the condition of $K_s \geq 1/(*[Br]_t)^2$ at the experimental minimum *[Br]$_t$.

Table 2. Comparison of calculated emf values[a] with the experimental values for the $CuCl_2$ system at 25˚C.

log *[Cl]$_t$	Calculated values (mV)			emf [found b](mV)
	emf$_{Cu}$	emf$_{Cl}$	emf$_{Cu}$ + emf$_{Cl}$	
−2.959	164.5	−0.2	164	165.7
−2.804	170.3	−0.4	170	169.7
−2.539	180.1	−1.2	179	176.6
−2.260	190.4	−3.9	186	186.8
−2.038	198.6	−9.1	189	191.0
−1.699	211.1	−24.7	186	186.2
−1.503	218.4	−37.0	181	179.5
−1.214	229.1	−57.1	172	171.7

[a]Calculated from the data of $CuCl_2$ in **Table 1**. [b]Emf vs. Ag/AgCl electrode.

electrode. In addition to the fact, the peak seems to shift into the lower log *[$CuSO_4$]$_t$ values in going from *[NaCl]$_t$/*[$CuSO_4$]$_t$ = 1 to 3. These facts also support the validity of the semi-theoretical treatment described above. Moreover, the Cu^{2+} electrode did not respond clearly aqueous solutions of NaCl (see the plot at the open triangles in **Figure 3**): the $-C'$ value analyzed by emf$_{Cl}$ was less than 8 mV/decade at R = 0.948. This fact indicates that the presence of only the Cl^- ion is not adequate for the potential response of the Cu^{2+}-selective electrode to Cl^-, namely, the response of the electrode to Cl^- needs the presence of Cu^{2+} in the test solutions. This result is not inconsistent with the presence of the $[Cl_2 = Cu\text{-}Y]^{2-}$ unit in the electrode process (2). Since a washing of the electrode with w resets the electrode potential into an initial condition, it can be supposed that an interaction of M^{2+} (or X_2M) with Y^{2-}(s) is weaker than or comparable with that of M^{2+} with H_2O. The same can be true of the Cd(II) system.

Using Equation (10a), we analyzed the plot at *[NaCl]$_t$/*[$CuSO_4$]$_t$ = 1 in the same manner. The A, B, C and log K_s values at R = 0.994 were 247 ± 5 mV, 24 ± 1 mV/decade, −21 ± 1 mV/decade, and 4.10 ± 0.09, respectively (see the curve in **Figure 3**). The log K_s value was the same as that for $CuCl_2$ within the experimental errors (see **Table 1**). Also, a difference in A between the mixture at *[NaCl]$_t$/*[$CuSO_4$]$_t$ = 1 and the aqueous solution of $CuCl_2$ was + 30 mV (= $A^{CuCl2} - A^{1:1}$). That is, the difference between the log $K_m(CuCl_2)$ and log K_m(1:1) values was 1.3_1 [= log $\{K_m(CuCl_2)/K_m(1:1)\} \approx (2 \times 0.030/0.05916) + \log 2$], where the $(\Delta\phi^0_{Y/Cu} + \Delta\phi^0_{Cl2CuY/Cl})$ term was assumed to be constant between the two systems. These facts suggest that the K_m value is dependent on the *[Cl]$_t$ value, while the K_s value is independent of the present *[Cl]$_t$ value at least. The strong *[Cl]$_t$-dependence of K_m can be easily supposed by the reaction (3) with the reaction of Cl^-, in other words, an increase in $[CuCl^+] + [Cl_2CuY^{2-}]_s$ in $[Cu]_t$ and/or $[Cl_2CuY^{2-}]_s$ in K_2, based on the relation $K_m = ([Cu]_t/*[Cu]_t)K_2$. On the other hand, the *[Cl]$_t$-dependence of K_s may be depressed by the presence of the $(D_{Cl}/g)^2$ term in K_s: $[Cl_2CuY^{2-}]_s/[Cu^{2+}](*[Cl]_t)^2 = K_s$ {see the above K_s definition at Equations (10) and (10a)}.

3.6. Application of the Present Model to Other Liquid Membrane ISEs

In the same manner as that (see **3.4**) for the potential responses measured by the commercial Ca^{2+} electrode, we analyzed data [5] reported by Morf and Simon for a potential response of the neutral carrier-based Ca^{2+} electrode with *o*-nitrophenyl octyl ether to an aqueous solution of $Ca(SCN)_2$. The A, B, C, and log K_s values at R = 0.998 were > (85 ± 5) mV, 18 ± 1 mV/decade, −22 ± 2 mV/decade, and 4.27 ± 0.22, respectively (from **Figure 1** in [5]). Also, data [7] reported by Egorov and Lushchik for the potential response of a H^+ electrode based on a neutral amine-type carrier in dioctyl phthalate-PVC membrane to the hydrofluoric acid solution was analyzed by using Equation (11): A > (233 ± 21) mV, B = 74 ± 7 mV/decade, C = −67 ± 5 mV/decade, and log K_s = 4.09 ± 0.19 at R = 0.991 (from **Figure 4** in [7]). The same values were obtained from the analysis with Equation (17) [7] proposed by them: emf = $A + B \log a_{H+} + (C/2) \log \{2K_{ex}(a_{H+})^2 + (K_{ex})^2(a_{H+})^4 + 1\}$ under the conditions of $a_{H+} = a_{F-}$ and $\overline{C}_{Am}^{tot} = \overline{C}_{R}^{tot}$ and then this equation is easily arranged into $A + B \log a_{H+} + C \log \{K_{ex}(a_{H+})^2 + 1\}$, being equivalent to Equation (11). Here, a_j (j = H^+, F^-), $\overline{C}_{Am}^{tot}$, and $\overline{C}_{R}^{tot}$ denote an activity of j in the test solution, total concentrations of amine (Am) and a lipophilic univalent anion R^- included in a liquid membrane, respectively. The term K_{ex} is an extraction constant ($mol^{-2}\cdot L^2$) of H^+F^- by Am into the liquid membrane and so corresponds to the K_s value in unit. At least, the results for the two Ca^{2+} electrodes suggest essential similarity in model between the solid-state membrane ISE and the liquid membrane ISE [7,9]. Also, a model suggesting the formation of X_2MY^{2-} in a liquid membrane has been proposed [12], where Y^{2-} means a basic ionophore. However, its detailed description was not found [12]. Furthermore, another model with the formation of XM^IY^-(s) in Equation (2) could reproduce the Λ-shaped plot at R = 0.983 for the above H^+ electrode. This R value was smaller than that (0.991) of the model with $X_2M^IY^{2-}$(s), showing the advantage of the X_2MY^{2-}(s) formation.

3.7. X^- Concentration at Peak Potential

The concentration ($*[X]_t^{peak}$) at the peak potential was estimated from the derivative of Equation (10) under the condition of $\frac{demf}{d\left(^*[X]_t\right)} = 0$, where $\frac{demf}{d\left(^*[X]_t\right)}$ = $B/*[X]_t + 2CK_s(*[X]_t)/\{1 + K_s(*[X]_t)^2\}$ and then $*[X]_t^{peak} = \sqrt{\frac{-B}{(B+2C)K_s}}$ {= 2($*[M]_t^{peak}$) for Equation (10a)}. The $*[X]_t^{peak}$ values were 2.6 × 10^{-4} and 0.010 mol L^{-1} for the CdI_2 and $CuCl_2$ systems, respectively. These values are in good agreement with those of the peaks shown in **Figures 1** and **2**. The same result was also obtained for the $Ca(SCN)_2$ system with the experimental log $*[Ca]_t^{peak}$ of about −2.5 [5]. Similarly, the log $*[HF]_t^{peak}$ value (= −2.0) was in good agreement with the experimental upper limit of the proton response [7]. These results indicate well the reproducibility of the plots based on Equations (10) and (11).

3.8. For Properties of the M^{2+} Electrodes Employed

The K_s values were calculated to be {$K_s(CdCl_2)$ <} $K_s(CdBr_2)$ < $K_s(CdI_2)$. This fact indicates that the selectivity of the Cd^{2+} electrode (Horiba, type 8007-10C with a solid-state membrane) against X^- is in the order $X^- = I^-$ < Br^- < Cl^-. The same is partly true of the Cu^{2+} electrode (type 8006-10C): $K_s(CuCl_2)$ << $K_s(CuBr_2)$ (**Table 1**). Predicting $[j]_s$ (j = Y^{2-}, X_2MY^{2-}) to be unity in Equation (4), then the −log K_s value can be proportional to the logarithmic solubility product, log K_{sp} [=log {$*[M^{2+}]$ $(*[X^-])^2$}]. From solubility (S) data [22] at 25˚C in w, the estimated values were in the orders CdI_2 {log (K_{sp}/mol^3 L^{-3}) = log $4S^3$ = 0.90_8} < $CdBr_2\cdot 4H_2O$ (1.16_2) < $CdCl_2\cdot(5/2)H_2O$ (1.73_9) and $CuBr_2$ (1.79_5) ≤ $CuCl_2\cdot 2H_2O$ (1.80_1), where it was assumed that 100 g of aqueous solutions equals 0.10_0 L and then the S data in a %(w/w) unit was converted to that in a mol L^{-1} one. This order suggests that the smaller the log $K_{sp}(MX_2)$ value is, the more easy MX_2 interacts with the electrode, and then the larger the interference of X^- against the electrode becomes. The same discussion can hold for the CaX_2 system with the liquid membrane, as follows. The log $K_{sp}(CaX_2)$ values in w at 25˚C were estimated to be 1.54_9 for $CaCl_2\cdot 6H_2O$, 1.48_2 for $CaBr_2\cdot 6H_2O$, 1.29_3 for $CaI_2\cdot 6H_2O$, and 1.86_5 for $Ca(NCS)_2\cdot 4H_2O$ from the S data [22]. The log K_{sp} order for X = Cl, Br and I was in good agreement with the −log K_s one, although the log $K_s(CaCl_2)$ value could not be determined. A deviation of the $Ca(SCN)_2$ system from the order suggests that an incorporation of Ca^{2+} in complex formation with the neutral carrier (L) around the test solution/liquid membrane-interface strongly contributes an increase in K_s, namely a transfer of CaL^{2+}, $XCaL^+$, X_2CaL and so on [8] into the o phase.

4. Conclusion

It was demonstrated that the present model based on the balances among the electrochemical potentials reproduce well the potential responses of the commercial Cd^{2+} and Cu^{2+} electrodes with the solid-state membranes in the presence of only the counter halide ions. Also, one could see that the phenomena for the Ca^{2+} and H^+ electrodes with the liquid membranes are similarly treated. These facts suggest that the present model contains essential processes being important for the potential responses of electrodes with liquid membranes at least. Further studies will be required for this agreement in potential response between the electrodes with the solid-state membranes and those with the liquid membranes, because the latter electrodes respond under the more-complicated experimental conditions. Not taking account of so-called interfering ions in the test solutions, Equations (10) and (10a) do not reach the general equations derived before. However, Equations (10) and (10a) could directly estimate the parameters, K_s and A (with K_m). By these equations, one can relate properties of the M^{2+} and M^+ electrodes with K_{sp}, although their applications are limited to the solid-state membrane ISEs showing the Λ-shaped potential responses.

5. References

[1] D. N. Hume, D. D. DeFord and G. C. B. Cave, "A Polarographic Study of the Cadmium Thiocyanate Complexes," *Journal of American Chemical Society*, Vol. 73, 1951, pp. 5323-5325. doi:10.1021/ja01155a094

[2] C. E. Vanderzee and H. J. Dawson Jr., "The Stability Constants of Cadmium Chloride Complexes: Variation with Temperature and Ionic Strength," *Journal of American Chemical Society*, Vol. 75, 1953, pp. 5659-5663. doi:10.1021/ja01118a056

[3] P. Gerding, "Thermochemical Studies on Metal Complexes I. Free Energy, Enthalpy, and Entropy Changes for Stepwise Formation of Cadmium(II) Halide Complexes in Aqueous Solution at 25˚C," *Acta Chimca Scandinavica*, Vol. 20, No. 1, 1966, pp. 79-94. doi:10.3891/acta.chem.scand.20-0079

[4] Y. Kudo, D. Todoroki, N. Horiuchi, S. Katsuta and Y. Takeda, "Ion-Pair Formation of Sodium Salts of Several Oxo Anions and Cadmium Halides in Water and the Distribution of Monovalent Sulfate Ion Pairs in Nitrobenzene," *Journal of Chemical and Engineering Data*, Vol. 55, No. 7, 2010, pp. 2463-2469. doi:10.1021/je900861h

[5] W. E. Morf and W. Simon, "Cation-Response Mechanism of Neutral Carrier Based Ion-Selective Electrode Membranes," *Helvetica Chimica Acta*, Vol. 69, 1986, pp. 1120-1131. doi:10.1002/hlca.19860690520

[6] E. Lindner, E. Gráf, Z. Niegreisz, K. Tóth, E. Pungor and R. P. Buck, "Responses of Site-Controlled, Plasticized Membrane Electrodes," *Analytical Chemistry*, Vol. 60, No. 4, 1988, pp. 295-301. doi:10.1021/ac00155a004

[7] V. V. Egorov and Y. F. Lushchik, "H^+-Selective Electrodes Based on Neutral Carriers: Specific Features in Behaviour and Quantitative Description of the Electrode Response," *Talanta*, Vol. 37, No. 5, 1990, pp. 461-469. doi:10.1016/0039-9140(90)80071-M

[8] Y. Kudo, Y. Kobayashi, S. Katsuta and Y. Takeda, "Ion-pair Formation of Cadmium-18-Crown-6 Ethers Complex Ions with Picrate and Chloride Ions in Water and Distribution of Its Picrate Ion-pair Complexes into Benzene," *Journal of Molecular Liquids*, Vol. 146, 2009, pp. 60-65. doi:10.1016/j.molliq.2009.02.004

[9] T. Kakiuchi and M. Senda, "The Theory of Liquid Ion Exchange Membrane Ion-Selective Electrodes Based on the Concept of the Mixed Ion-Transfer Potential," *Bulletin of the Chemical Society of Japan*, Vol. 57, No. 7, 1984, pp. 1801-1808. doi:10.1246/bcsj.57.1801

[10] A. Jyo, K. Fukamachi, W. Koga and N. Ishibashi, "The Influence of a Co-ion on the Potential of a Liquid -Exchanger Membrane Electrode," *Bulletin of the Chemical Society of Japan*, Vol. 50, No. 3, 1977, pp. 670-672. doi:10.1246/bcsj.50.670

[11] P. Bühlmann and Y. Umezawa, "Apparently 'Non-Nernstian' Equilibrium Responses Based on Complexation Between the Primary Ion and a Secondary Ion in the Liquid ISE Membrane," *Electroanalysis*, Vol. 11, No. 10-11, 1999, pp. 687-693. doi:10.1002/(SICI)1521-4109(199907)11:10/11<687::AID-ELAN687>3.0.CO;2-C

[12] S. Amemiya, P. Bühlmann and K. Odashima, "A Generalized Model for Apparently 'Non-Nernstian' Equilibrium Responses of Ionophore-Based Ion-Selective Electrodes. 1. Independent Complexation of the Ionophore with Primary and Secondary Ions," *Analytical Chemistry*, Vol. 75, No. 14, 2003, pp. 3329-3339. doi:10.1021/ac026471g

[13] G. D. Christian, "Analytical Chemistry," 5th Edition, John Wiley & Sons, New York, 1994, p. 335.

[14] Y. Kudo, R. Fujihara, T. Ohtake, S. Katsuta and Y. Takeda, "Evaluation of the Hydrophilic Property of Sodium Ion-Pair Complexes with 3*m*-Crown-*m* Ethers (*m* = 5, 6) and Their Benzo-Derivatives by Solvent Extraction," *Analytical Sciences*, Vol. 24, 2008, pp. 999-1003. doi:10.2116/analsci.24.999

[15] Y. Kudo, S. Takeuchi, Y. Kobayashi, S. Katsuta and Y. Takeda, "Potentiometric Determination of Ion-Pair Formation Constants for Cadmium, Calcium Salts, and Cadmium-18-Crown-6 Ether Derivative Complexes with a Sulfate Ion in Water," *Journal of Chemical and Engineering Data*, Vol. 52, No. 5, 2007, pp. 1747-1752. doi:10.1021/je700135j

[16] S. Wasylkiewicz, "Ion Association in Aqueous Solutions of Electrolytes. II. Mathematical Model for Sulphates of Bivalent Metals," *Fluid Phase Equilibria*, Vol. 57, 1990, pp. 277-296. doi:10.1016/0378-3812(90)85127-V

[17] T. Kakiuchi, "Limiting Behanior in Equilibrium Partitioning of Ionic Components in Liquid-Liquid Two-Phase Systems," *Analytical Chemistry*, Vol. 68, No. 20, 1996, pp. 3658-3664. doi:10.1021/ac960032y

[18] Internet Available: http://www.horiba.com/us/en/application/material-property-characterization/water-analysis/water-quality-electrochemistry-instrumentation/electrodes/ion-electrodes/details/copper-ion-electrode-8006-10c-9511/

[19] Internet Available: http://www.horiba.com/us/en/application/material-property-characterization/water-analysis/water-quality-electrochemistry-instrumentation/electrodes/ion-electrodes/details/cadmium-ion-electrode-8007-10c-9515/

[20] Internet Available: http://www.horiba.com/us/en/application/material-property-characterization/water-analysis/water-quality-electrochemistry-instrumentation/electrodes/ion-electrodes/details/calcium-ion-electrode-8203-10c-9587/

[21] A. J. Bird and L. R. Faulkner, "Electrochemical Methods: Fundamentals and Applications," 2nd Edition, John Wiley & Sons, New York, 2001, pp. 60-62; 74-81.

[22] K. A. Inaba, S. Takagi, K. Tajima, H. Tohara, K. Nakatsuka, K. Nakanishi, H. Nakayama, T. Makita and M. Muramatsu, "Handbook of Chemistry, Fundamentals II", In: H. Chihara, Ed., 3rd Edition, *The Chemical Society of Japan*, Maruzen, Tokyo, 1984, pp. II-166; II-177.

